Advances in Nanoparticles, 2016, 5, 140-148
Published Online May 2016 in SciRes. http://www.scirp.org/journal/anp
http://dx.doi.org/10.4236/anp.2016.52016

High Sensitivity of Porous Cu-Doped SnO_2 Thin Films to Methanol

Sara Benzitouni[1*], Mourad Zaabat[1], Aicha Khial[1], Djamil Rechem[1], Ahlem Benaboud[1], Dhikra Bouras[1], Abdelhakim Mahdjoub[2], Mahdia Toubane[3], Raphael Coste[4]

[1]Laboratoire des Composants Actifs et Matériaux (LCAM), Université Larbi Ben M'hidi, Oum El Bouaghi, Algérie
[2]Laboratoire des Matériaux et Structure des Systèmes Electromécaniques et leur Fiabilité (LMSSEF), Université Larbi Ben M'hidi, Oum El Bouaghi, Algérie
[3]Unité de Recherche Matériaux, Procédés et Environnement (URMPE), Université M'hamed Bougara, Boumerdes, Algérie
[4]Laboratoire de Recherche en Nanoscience (LRN), UFR Sciences, Université de Reims, Reims, France
Email: *benzitouni.sarah@univ-oeb.dz, *sarahnano@hotmail.fr

Received 27 March 2016; accepted 17 May 2016; published 20 May 2016

Abstract

Porous Cu-doped SnO_2 thin films were synthesized by the sol-gel dip-coating method for enhancing methanol sensing performance. The effect of Cu doping concentration on the SnO_2 sensibility was investigated. XRD data confirm that the fabricated SnO_2 films are polycrystalline with tetragonal rutile crystal structure. AFM and SEM micrographs confirmed the roughness and the porosity of SnO_2 surface, respectively. UV-Vis spectrum shows that SnO_2 thin films exhibit high transmittance in the visible region ~95%. The band gap (3.80 - 3.92 eV) and the optical thickness (893 - 131 nm) of prepared films were calculated from transmittance data. The sensing results demonstrate that SnO_2 films have a high sensitivity and a fast response to methanol. In particular, 3% Cu-SnO_2 films have a higher sensitivity (98%), faster response (10^{-2} s) and shorter recovery time (18 s) than other films.

Keywords

SnO_2, Cu-Doped, Sensitivity, Porosity, Response Time, Band Gap, Thin Films

1. Introduction

In recent years, the detection methods of toxic chemical species and measurement of their concentration in-

*Corresponding author.

How to cite this paper: Benzitouni, S., Zaabat, M., Khial, A., Rechem, D., Benaboud, A., Bouras, D., Mahdjoub, A., Toubane, M. and Coste, R. (2016) High Sensitivity of Porous Cu-Doped SnO_2 Thin Films to Methanol. *Advances in Nanoparticles*, **5**, 140-148. http://dx.doi.org/10.4236/anp.2016.52016

creased significantly. This interest is mainly due to environmental considerations [1]-[5]. In the field of detection of chemical species, we must distinguish chemical sensors and in particular micro-sensors and micro-devices that play a critical role in environmental monitoring and environmental control (air, water), facilitating a better quality of life. The projected increase in global energy usage and unwanted release of pollutants has led to a serious focus on advanced monitoring technologies for environmental protection. Much research has been focused on the development of highly accurate sensors, highly sensitive and reliable. Shipping devices ever smaller micro-level have capabilities to control the nanomaterials such as: biological, chemical and pathological samples [6] [7]. In this context, the study focuses on the detection of methanol, which has strong toxicity, and can cause death because of its depressant properties on the central nervous system and blood system.

The metal oxides are widely used as micro-sensors due to their unique surface properties, particularly having a large active surface area, which can make the ideal detection elements such as: Co_3O_4 [7], Ag_2O [8], PPC/NC [9], CuO [10], α-MnO_2 [11] and SnO_2 [12]. Among of all metal oxide semiconductors, SnO_2 is a proper candidate for potential application in chemical sensing due to its thermal/chemical stability, good oxidation resistance with wide band gap energy of 3.6 eV. Up to now, few strategies have been adopted to improve the performance of SnO_2 sensors by introducing various dopants such as Ni, Fe and Pt [12]-[14], or by varying the experimental conditions on the SnO_2 fabrication such as [15] [16]. In this paper, the effect of Cu doping concentration on the SnO_2 sensibility is investigated that has not reported in the literature as nano-sensor. The Cu^{2+} have smaller ionic radius than Sn^{4+}, so Cu^{2+} can be incorporated onto the SnO_2 lattice simply by replacing Sn^{4+}. This may be leading to form more oxygen vacancies, which improves chemical sensing properties of Cu-doped SnO_2 thin films.

2. Experimental Procedure

2.1. Materials

Tin (II) chloride dihydrate 98% |$SnCl_2$, $2H_2O$|, copper (II) acetate monohydrate 98% |$Cu(CH_3COO)_2$, H_2O)|, absolute ethanol ≥99.8% |C_2H_5OH| and hydrochloric acid 36% |HCl| were used to preparing undoped and Cu-doped SnO_2 thin films as a chemical-sensors for enhancing methanol sensing performance 99.8% |CH_3OH|. "All products are from Sigma-Aldrich".

2.2. Preparation of Undoped and Cu-Doped SnO_2 Thin Films

Undoped and Cu-doped SnO_2 thin films were prepared by the sol-gel dip-coating method using materials mentioned previously. Tin (II) chloride dihydrate [$SnCl_2$, $2H_2O$] as a precursor and copper (II) acetate monohydrate [$Cu(CH_3COO)_2$, H_2O] as a dopant source were dissolved at the same time in absolute ethanol with a total molarity of 0.4M. The Sn-O bonds were necessary for the formation of SnO_2 films, which are obtained by the hydrolysis reaction between the Tin and the solvent. This reaction is usually accelerated by acidic catalysts. So, a few drops of HCl are added to the mixture to obtain a clear and homogeneous solution, the blue mixture was stirred at 70˚C for 2.30 h. It was usually prepared one day before using. The glass substrates were cleaned in an ultrasonic bath in acetone, ethanol and distilled water successively. The layers were deposited by immersing a substrate in the solution for 1 min (Dip-coater KSVDCX2) and then dried at high temperature 300˚C for 4 min in an electric furnace (Nabertherm B-180). The procedure from immersing to drying was repeated 15 times, the films were then annealed at 550˚C for 1 h. To investigate the effect of copper doping concentration on the physical and sensing properties of SnO_2, tin oxide thin films were fabricated at several concentrations of Cu: (0% Cu, 3% Cu, and 6% Cu).

2.3. Sensors Characterization

The structural characterization of the films was performed using X-ray diffractometer [type Bruker AXS-8D with CuK_α 1.54056 Å]. The surface morphology was studied using atomic force microscopy (A100 model of APE Research) and Scanning Electron Microscopy (LEO Gemini 98). The optical properties were investigated using a spectrophotometer UV-Vis (Jasko V-630). The sensing properties of the films were studied by Keithley source meter (model 2401, made in China).

2.4. Chemical Sensors Testing

In order to study the sensibility of SnO_2 thin films, we manufactured electrical contacts separately with 1 cm

spacing by silver lacquer on their surface. Then, the electrical contacts were covered by a plastic insulator to avoid their response during methanol injection. Finally, we kept the sample in the water and then connected to an electrical circuit Keithley source meter (model 2401, made in China) and controlled with a computer (NI LabView software). After equilibrium and stability of sample resistivity in water, we injected the methanol. Data acquisition card collected the resistance values across the chemical sensor in real-time and displayed on a computer. The applied voltage is estimated at 1.0 Volt. In order to determine the effect of Cu doping concentration on the SnO_2 sensibility, the sensor responses (S) were calculated by the injection of 1.0 M of methanol using Equation (1). All electrical measurements were performed at room temperature.

$$S = \Delta R / R_w \times 100 \tag{1}$$

where R_w is the resistance in water and ΔR is the variation of resistance during injection of chemical liquid.

3. Results and Discussion

3.1. Structural Properties

Figure 1(a) shows the X-ray diffraction patterns of undoped and Cu-doped SnO_2 thin films. The data reveal that all peaks: 26.52˚ (110), 33.73˚(101), 37.83˚(200), 44.10˚(210) and 51.73˚(211) correspond to the planes of tetragonal rutile crystalline phases of tin oxide [JCPDS card (41-1445)]. And no peak of other crystalline phases was detected, which is probably due to the low content of Cu-dopant. These results are similar to those reported in some publication [17]-[21], but another peak has appeared and more intense in our study at 44.10˚(210). It can be seen that the intensity of a dominant peak (210) among of all other peaks decreases with increasing doping concentration, indicating the slight deterioration of crystallinity of SnO_2, which may be due to the formation of stress; a contraction in the lattice because of substitution of copper [Cu^{2+}: 0.73Å] on the tin [Sn^{4+}: 0.83Å] sites. The crystalline size of SnO_2 Equation (2) and the dislocation density Equation (3) have been calculated [22] and reported in **Table 1** respectively.

$$D = 0.9\lambda / \beta \cos\theta \tag{2}$$

$$\delta = 1/D^2 \tag{3}$$

where λ is the X-ray wavelength, β is the full width at half maximum of the XRD peak, θ is the Bragg diffraction angle. The increase in the dislocation density (δ) in the system suggests that the doping has induced defects in the system.

3.2. Morphological Properties

The surface morphology of samples was analyzed by SEM and AFM respectively. **Figure 2** shows the scan-

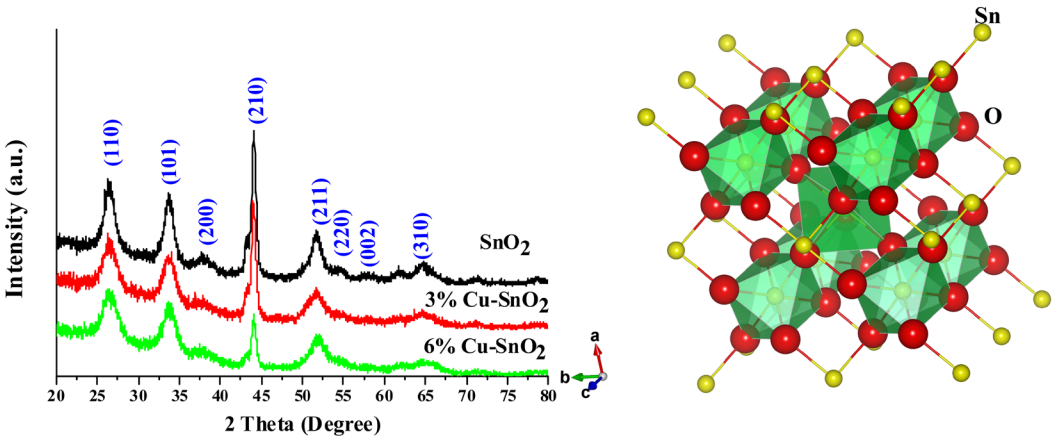

(a) (b)

Figure 1. (a) XRD patterns of undoped and Cu-doped SnO_2 thin films and (b) Unit cell structure of rutile SnO_2 with polyhedral representation, drawn with VESTA 2.x.

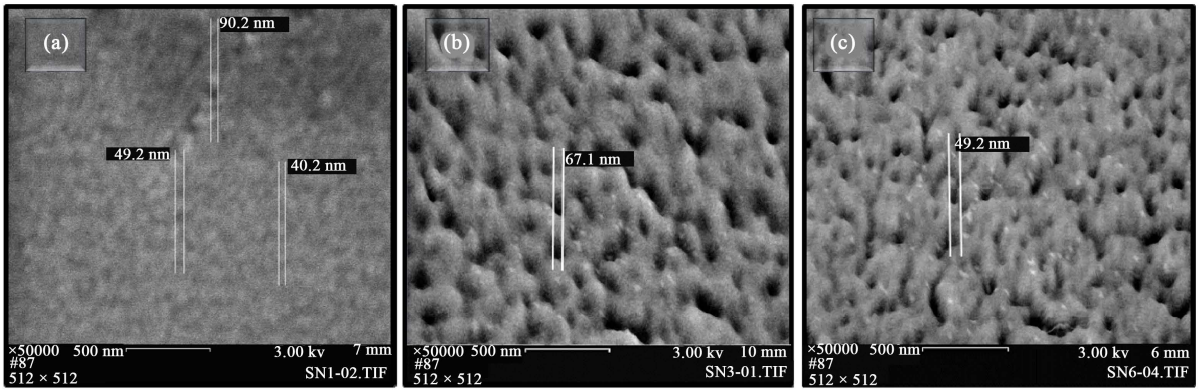

Figure 2. SEM micrographs of SnO_2 thin films deposited by sol-gel dip-coating method. (a) Undoped SnO_2; (b) 3% Cu-doped SnO_2 and (c) 6% Cu-doped SnO_2 thin films.

Table 1. The XRD, AFM and transmittance analysis.

samples	FWMH (210) (°)	(D) Crystal size (nm)	(δ) Dislocation density (nm^{-2}) $\times 10^{-3}$	(E_g) Band gap (eV)	(d) Thickness (nm)	(RMS) roughness (nm)	(D_p) Grain size (nm)	(S) Specific surface area (cm^2/g) $\times 10^7$
SnO_2	0.480	17.86	3.13	3.88	893	30.80	93	9.41
3% Cu-SnO_2	0.494	17.36	3.31	3. 95	744	19.60	72	12.16
6% Cu-SnO_2	0.579	14.79	4.57	4.00	131	08.97	46	19.04

ning electron micrographs (SEM) of undoped and Cu-doped SnO_2 thin films. It is evident that the films are uniform with granular surface nanostructures. For undoped SnO_2 (**Figure 2(a)**), the grains are almost spherical in shape and their diameter size is approximately in the range (50 - 90 nm). For Cu-doped SnO_2 (**Figure 2(b)**), we can see that the samples presented a three-dimensional random arrangement of nanoropores with an average pore diameter about of (49 - 67 nm). Therefore, the surface morphology of films is strongly depending upon the Cu doping concentration. Inspired by this idea, the porous structure is believed to facilitate the transport of reactant molecules and to enhance chemical-sensing performance.

Avoid The dependence of the grain size and the RMS roughness as a function of Cu doping concentration was revealed by statistical processing of 2D/3D of AFM images that showed in **Figure 3** using [Gwyddion 2, 34]. The grain size of particles D_p and the RMS roughness parameters are reported in **Table 1**. From this table, we observed that both the grain size (93 to 46 nm) and the RMS roughness (30.8 to 8.97 nm) were decreased with increasing cu doping concentration.

The total surface area per unit of mass or bulk volume or cross sectional area is known as specific surface area. This material property of solids has an important role in the process of adsorption, heterogeneous catalysis and reactions on surfaces. It can be measured using the formula of Equation (4) [23]

$$S = 6 \times 10^3 / \rho D_p \tag{4}$$

where S is the specific surface area, D_p is the size of the particle and ρ is the density of SnO_2 (6.85 g/cm^3). **Table 1** shows that the specific surface area increased with increasing copper doping concentration. Therefore, the possibility to accelerate the reaction on the SnO_2 surface is increased.

3.3. Optical Properties

Figure 4 shows the optical transmission spectra of undoped and Cu-doped SnO_2 thin films. We can distinguish in this figure the presence of a high transparency in the range of wavelength [400 - 1100 nm], where the high transmittance of these films was about of 95%. However, we observe a sharp decrease in the transmittance with increasing Cu doping concentration. In this wavelength range, we can also observe the interference fringes due to multiple reflections on the different interfaces, which indicate that the films prepared under these conditions

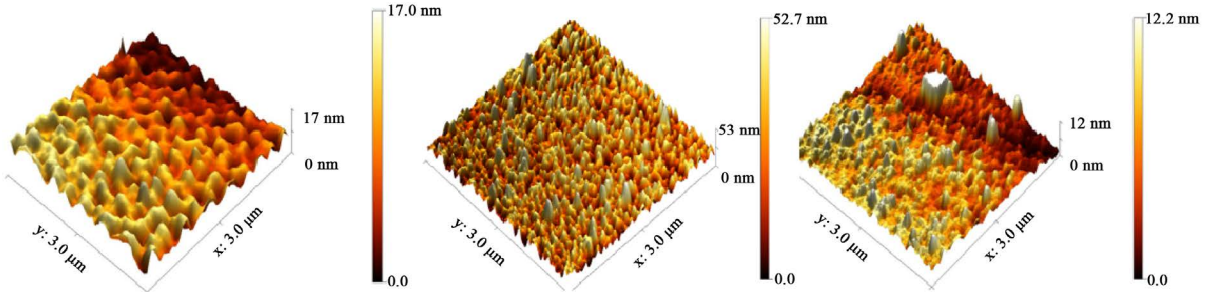

(a) (b) (c)

Figure 3. AFM micrographs (3D) of SnO_2 thin films deposited by sol-gel dip-coating method. (a) Undoped SnO_2; (b) 3% Cu-doped SnO_2 and (c) 6% Cu-doped SnO_2 thin films.

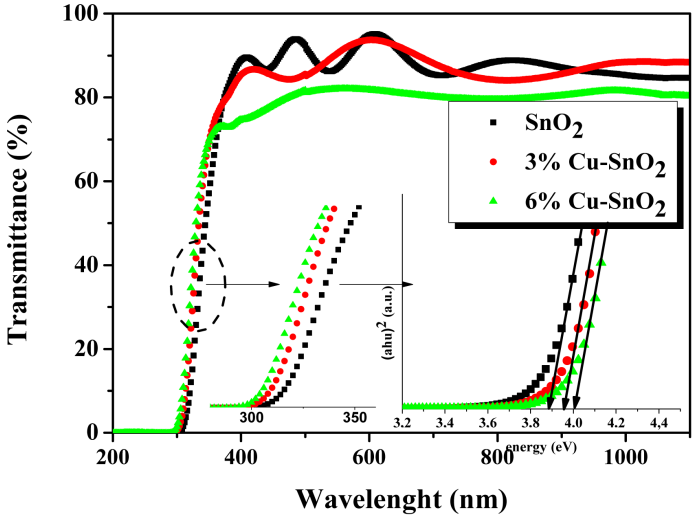

Figure 4. UV-Vis transmission spectra of undoped and Cu-doped SnO_2 thins films, and spectral dependence of the absorption coefficient $(\alpha h\upsilon)^2 = f(h\upsilon)$ for SnO_2 thin films.

are smooth and uniform [24]. In addition, the optical absorption edge was shifted towards a shorter wavelength region with increasing Cu doping concentration, which was attributed to the Burstein-Moss effect [25].

The band gap energy is calculated on the basis of the maximum absorption band of SnO_2 nanosheet materials Equation (5). The plots of $(\alpha h\upsilon)^2$ as a function of energy $(h\upsilon)$ for Cu doped SnO_2 films tend asymptotically towards a linear section, which show that the investigated films have a direct optical band gap [26] [27].

$$\alpha = A/h\nu\sqrt{h\upsilon - E_g} \tag{5}$$

where A is a constant, $h\upsilon$ is the photon energy and E_g is the optical band gap. The optical band gap of our films was found increased with increasing Cu concentration from 3.88 to 4.00 eV. This indicates that the copper was correctly incorporated into the SnO_2 structure.

The thickness of the deposited films is obtained by fitting the transmittance experimental spectra by the theoretical model as shown in **Figure 5** using Swanepoel formulation of the transmittance and the Forouhi-Bloomer description of optical indices [28] [29]. As can be seen, the optical thickness decreases when the doping concentration increases from 893 nm to 131 nm. The decreasing in the thickness may be due to distortions in the SnO_2 lattice and the decrease its parameters following the introduction of the Cu with an ionic radius smaller than of Sn.

3.4. Methanol Detection Using SnO_2 Thin Films-Sensors

The potential application of SnO_2 thin films as chemical sensors was investigated for detection of hazardous and

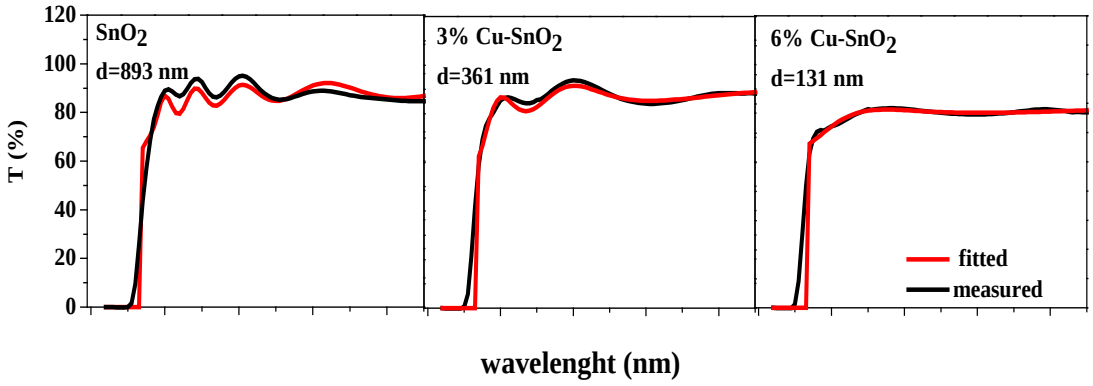

Figure 5. Experimental and fitted spectra of transmittance, corresponding to undoped and Cu-doped SnO_2 thin films.

toxic chemical species as a methanol, which are not environmentally friendly. The reason of phenomenon is that the resistance R of SnO_2 thin films widely changed when the aqueous methanol was adsorbed. Therefore, methanol detection using SnO_2 thin films-sensors was performed by measuring the resistance as a function of time R (t), which is shown in **Figure 6(a)**. This figure shows in the one hand a significant response which is clearly demonstrated by the change in the resistance of undoped and Cu-doped SnO_2 thin films. On the other hand, the SnO_2 thin films become more sensitive with a fast response in the presence of copper, this may be due to their unique surface properties such as a high surface area and a high pore density of surface, which facilitate the transport of reactant molecules and to enhance chemical-sensing performance. The sensing parameters of our films are also schematized in the **Figure 6(b)**. As it can be seen, the sensitivity of SnO_2 films increases with increasing Cu doping concentration from 77.34% to 98.7%. However, the sensitivity of 3%Cu-SnO_2 films (98.7%) is greater than the sensitivity of 6% Cu-SnO_2 films (92.75%), this may be due to the deactivation of the surface area of SnO_2 with doping by 6%Cu. Besides, 3%Cu-SnO_2-films shows a fast response time (10^{-2} s) and a short recovery time (18 s) than other samples. The main influence of doping process is also for enhancing the electrical properties. It's well known that, chem-sensing properties are improved in the case of doped materials, mixed materials, etc. This process leads to an increase of the electron concentration, which eventually increases the oxygen vacancies-related defects in SnO_2 nanoparticles. Therefore, more adsorption sites for liquid molecules are provided by these oxygen vacancies causing the surface to become highly active for a reaction, so that the sensing properties are improved. In the other hand, the porosity of the Cu doped SnO_2 surface observed by means of SEM images can be improved the flow of generated electrons. The many responses of 6% Cu-doped SnO_2 films to the methanol at the same test (**Figure 6(c)**) confirming the reliability of Cu-SnO_2 sensors.

The chemical sensing mechanism of SnO_2 thin films to methanol can be explained in **Figure 7** with according to the following equations:

The dissolved oxygen is converted to ionic species (such as O_2^- and O^-), which has gained electrons from the SnO_2 conduction band, Equation (6) [8] [13].

$$O_{2(diss)} \rightarrow O_{2(ads)}$$

$$O_{2(ads)} + e^- \rightarrow O_2^-$$

$$O_2^- + e^- \rightarrow 2O^- . \quad (6)$$

The reaction between methanol and ionic oxygen species is executed by two different ways Equation (7) and Equation (8) [30].

$$CH_3OH_{(Liq)} + O^- \rightarrow HCHO + H_2O + e^- \quad (7)$$

$$HCHO + 2O_{(bulk)} \rightarrow HCOOH + O_{(vac)}$$

$$CH_3OH_{(Liq)} + O_{2(ads)}^- \rightarrow HCOOH + H_2O + e^- . \quad (8)$$

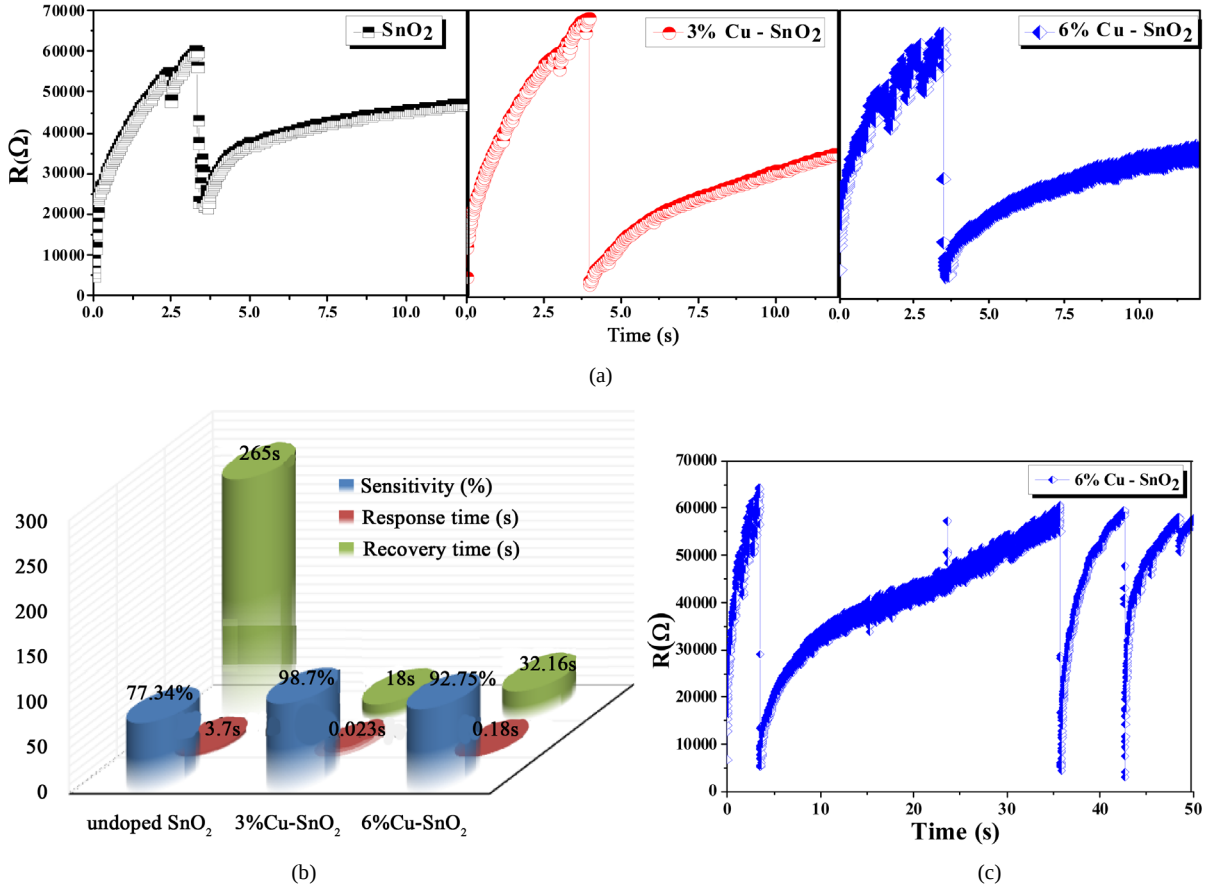

Figure 6. (a) The electrical resistance of undoped and Cu-doped SnO_2 thin films-sensors (0, 3, 6 wt%) as a function of time with exposure 1.0 M to methanol liquid, (b) Effect of Cu doping concentration on the sensing parameters of SnO_2: sensitivity, response time and recovery time and (c) The many responses of 6% Cu-doped SnO_2 films to the methanol at the same test.

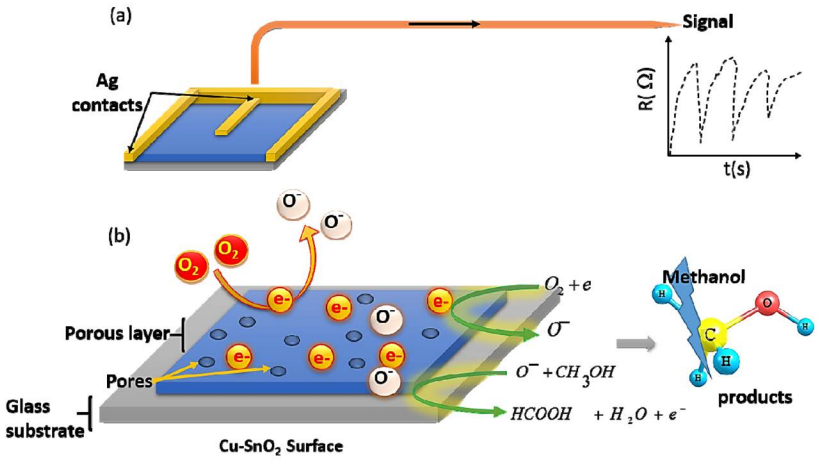

Figure 7. Schematic view of: (a) sensor contact and (b) reaction mechanism of methanol in presence of SnO_2 thin films.

4. Conclusion

In this paper, the undoped and Cu-doped SnO_2 thin films were synthesized by the sol-gel method. The various measurement equipments were used to characterize their structural, morphological and optical properties. The

changes in resistance of undoped and Cu-doped SnO_2 thin films during the injection of methanol in aqueous solution show a high sensitivity in a very short time. The copper effect for developing the SnO_2 films as nano-sensor has been successfully realized. In particular, the 3% Cu-SnO_2 films have a higher sensitivity (98%), faster response (10^{-2} s) and shorter recovery time (18 s) than other films. We believed that it is a possible and effective route to improve the sensing performance of the thin films, as nano-sensors.

Acknowledgements

Laboratoire des Composants Actifs et Matériaux (LCAM), Université d'Oum El Bouaghi 04000, Algérie, have supported this work. The authors are grateful to the Algerian MESRS (Ministère de L'Enseignement Supérieur et de la Recherche Scientifique) for the financial support. S. Benzitouni thanks particularly the laboratory of Research of Nanoscience (LRN) for the SEM measurements and Unite of Research Materials, Processes and Environment (URMPE) for XRD measurements.

References

[1] Giaouris, E., Heir, E., Hébraud, M., Chorianopoulos, N., Langsrud, S., Møretrø, T., Habimana, O., Desvaux, M., Renier, S. and Nychas, G.-J. (2014) Attachment and Biofilm Formation by Foodborne Bacteria in Meat Processing Environments: Causes, Implications, Role of Bacterial Interactions and Control by Alternative Novel Methods. *Meat Science*, **97**, 298-309. http://dx.doi.org/10.1016/j.meatsci.2013.05.023

[2] Hernandez, M., Kapetanakou, A.-E. and Kucht, T. (2015) Environmental Sampling for *Listeria monocytogenes* Control in Food Processing Facilities Reveals Three Contamination Scenarios. *Food Control*, **51**, 94-107. http://dx.doi.org/10.1016/j.foodcont.2014.10.042

[3] Sivashankar, R., Sathya, A.-B., Vasantharaj, K. and Sivasubramanian, V. (2014) Magnetic Composite an Environmental Super Adsorbent for Dye Sequestration—A Review. *Environmental Nanotechnology, Monitoring & Management*, **1-2**, 36-49.

[4] García, V., Pongrácz, E., Phillips, P.-S. and Keiski, R.-L. (2013) From Waste Treatment to Resource Efficiency in the Chemical Industry: Recovery of Organic Solvents from Waters Containing Electrolytes by Pervaporation. *Journal of Cleaner Production*, **39**, 146-153. http://dx.doi.org/10.1016/j.jclepro.2012.08.020

[5] Plumlee, G.S., Morman, S.A., Meeker, G.P., Hoefen, T.M., Hageman, P.L. and Wolf, R.E. (2014) The Environmental and Medical Geochemistry of Potentially Hazardous Materials Produced by Disasters. Treatise on Geochemistry (Second Edition), 9, 257-304.

[6] Umar, A., Rahman, M.M., Kim, S.H. and Hahn, Y.B. (2008) Zinc Oxide Nanonail Based Chemical Sensor for Hydrazine Detection. *Chemical Communications*, No. 2, 166-168. http://dx.doi.org/10.1039/B711215G

[7] Rahman, M.M., Jamal, A., Khan, S.B. and Faisal, M. (2011) Fabrication of Highly Sensitive Ethanol Chemical Sensor Based on Sm-Doped Co3O4 Nano-Kernel by Solution Method. *The Journal of Physical Chemistry C*, **115**, 9503-9510. http://dx.doi.org/10.1021/jp202252j

[8] Rahman, M.-M., Khan, S.-B., Jamal, A., Faisal, M. and Asiri, A.M. (2012) Fabrication of Highly Sensitive Acetone Sensor Based on Sonochemically Prepared as-Grown Ag_2O Nanostructures. *Chemical Engineering Journal*, **192**, 122-128. http://dx.doi.org/10.1016/j.cej.2012.03.045

[9] Khan, S.-B., Akhtar, K., Rahman, M.-M., Asiri, A.-M., Seo, J., Alamry, K.-A. and Han, H. (2012) A Thermally and Mechanically Stable Eco-Friendly Nanocomposite for Chemical Sensor Applications. *New Journal of Chemistry*, **36**, 2368-2375. http://dx.doi.org/10.1039/c2nj40549k

[10] Khan, S.-B., Faisal, M., Rahman, M.-M., Abdel-Latif, I.-A., Ismail, A.-A., Akhtar, K., Al-Hajry, A., Asiri, A.-M. and Alamry, K.-A. (2013) Highly Sensitive and Stable Phenyl Hydrazine Chemical Sensors Based on CuO Flower Shapes and Hollow Spheres. *New Journal of Chemistry*, **37**, 1098. http://dx.doi.org/10.1039/c3nj40928g

[11] Wu, J., Wang, Q., Umar, A., Sun, S., Huang, L., Wang, J. and Gao, Y. (2014) Highly Sensitive P-Nitrophenol Chemical Sensor Based on Crystalline a-MnO_2 Nanotubes. *New Journal of Chemistry*, **38**, 4420. http://dx.doi.org/10.1039/C4NJ00420E

[12] Rahmana, M.-M., Jamala, A., Bahadar Khanb, S. and Faisal, M. (2011) Highly Sensitive Ethanol Chemical Sensor Based on Ni-Doped SnO_2 Nanostructure Materials. *Biosensors and Bioelectronics*, **28**, 127-134. http://dx.doi.org/10.1016/j.bios.2011.07.024

[13] Rahman, M.-M., Khan, S.-B., Jamal, A., Faisal, M. and Asiria, A.-M. (2012) Fabrication of a Methanol Chemical Sensor Based on Hydrothermally Prepared-Fe2O3 Codoped SnO_2 Nanocubes. *Talanta*, **95**, 18-24. http://dx.doi.org/10.1016/j.talanta.2012.03.027

[14] Jana, S., Mondal, G., Mitra, B.-C., Bera, P. and Mondal, A. (2014) Synthesis, Characterization and Electrocatalytic Activity of SnO2, Pt-SnO_2 Thin Films for Methanol Oxidation. *Chemical Physics*, **439**, 44-48. http://dx.doi.org/10.1016/j.chemphys.2014.05.003

[15] Zhang, B., Fu, W., Li, H., Fu, X., Wang, Y., Bala, H., Wang, X., Sun, G., Cao, J. and Zhang, Z. (2016) Synthesis and Characterization of Hierarchical Porous SnO_2 for Enhancing Ethanol Sensing Properties. *Applied Surface Science*, **363**, 560-565. http://dx.doi.org/10.1016/j.apsusc.2015.12.042

[16] Majumdar, S. (2015) The Effects of Crystallite Size, Surface Area and Morphology on the Sensing Properties of Nanocrystalline SnO_2 Based System. *Ceramics International*, **41**, 14350-14358. http://dx.doi.org/10.1016/j.ceramint.2015.07.068

[17] Mariammal, R.N., Ramachandran, K., Renganathan, B. and Sastikumar, D. (2012) On the Enhancement of Ethanol Sensing by CuO Modified SnO_2 Nanoparticles Using Fiber-Optic Sensor. *Sensors and Actuators B*: *Chemical*, **169**, 199-207. http://dx.doi.org/10.1016/j.snb.2012.04.067

[18] Chetri, P. and Choudhury, A. (2015) Investigation of Structural and Magnetic Properties of Nanoscale Cu Doped SnO_2: An Experimental and Density Functional Study. *Journal of Alloys and Compounds*, **627**, 261-267. http://dx.doi.org/10.1016/j.jallcom.2014.11.204

[19] Talebiann, N. and Jafarinezhad, F. (2013) Morphology-Controlled Synthesis of SnO_2 Nanostructures Using Hydrothermal Method and Their Photocatalytic Applications. *Ceramics International*, **39**, 8311-8317. http://dx.doi.org/10.1016/j.ceramint.2013.03.101

[20] Lee, G.-H. (2015) Effect of the N_2/O_2 Ratio on the Morphology of SnO_2 Crystals Synthesized through the Thermal Vaporation of Sn. *Ceramics International*, **41**, 12058-12064. http://dx.doi.org/10.1016/j.ceramint.2015.06.021

[21] Li, X., Deng, R., Li, Y.F., Yao, B., Ding, Z.H., Qin, J.M. and Liang, Q.C. (2016) Effect of Mg Doping on Optical and Electrical Properties of SnO_2 Thin Films: An Experiment and First-Principles Study. *Ceramics International*, **42**, 5299-5303. http://dx.doi.org/10.1016/j.ceramint.2015.12.059

[22] Cullity, B.D. (1978) Elements of X-Ray Diffractions. Addison-Wesley, Reading, 102.

[23] Divya, N.K. and Pradyumnan, P.P. (2016) Solid State Synthesis of Erbium Doped ZnO with Excellent Photocatalytic Activity and Enhanced Visible Light Emission. *Materials Science in Semiconductor Processing*, **41**, 428-435. http://dx.doi.org/10.1016/j.mssp.2015.10.004

[24] Studenikin, S.A., Golego, N. and Cocivera, M. (1998) Fabrication of Green and Orange Photoluminescent, Undoped ZnO Films Using Spray Pyrolysis. *Journal of Applied Physics*, **83**, 2104. http://scitation.aip.org/content/aip/journal/jap/84/4/10.1063/1.368295

[25] Kamat, P.-V. and Dimitrijevic, N.-M. (1989) Dynamic Burstein-Moss Shift in Semiconductor Colloids. *The Journal of Physical Chemistry*, **93**, 2873-2875. http://dx.doi.org/10.1021/j100345a003

[26] Pankove, J.I. (1971) Optical Processes in Semiconductors. Prentice-Hall Inc., Englewood Cliffs.

[27] Tauc, J. (1974) Amorphous and Liquid Semiconductors. Plenum Press, New York.

[28] Forouhi, A.R. and Bloomer, I. **(**1986) Optical Dispersion Relations for Amorphous Semiconductors and Amorphous Dielectrics. *Physical Review B*, **34**, 7018. http://dx.doi.org/10.1103/PhysRevB.34.7018

[29] Ilican, S., Caglar, M. and Caglar, Y. (2007) Determination of the Thickness and Optical Constants of Transparent Indium-Doped ZnO Thin Films by the Envelope Method. *Materials Science-Poland*, **25**, 709-718.

[30] Patel, N.G., Patel, P.D. and Vaishnav, V.S. (2003) Indium Tin Oxide (ITO) Thin Film Gas Sensor for Detection of Methanol at Room Temperature. *Sensors and Actuators B*: *Chemical*, **96**, 180-189. http://dx.doi.org/10.1016/S0925-4005(03)00524-0